行政院國家科學委員會專題研究計畫成果報告

影響 $RM_xBa_{2-x}Cu_3O_{7-\delta}$ (R = Nd, Eu; M = Ca, Sr) 系列化合物超導性的參數

The Parameters Affecting the Superconductivity of $RM_xBa_{2-x}Cu_3O_{7-\delta}$ (R = Nd, Eu; M = Ca, Sr) Compounds

計畫編號：NSC87-2113-M-032-007

執行期限：自民國 86 年 8 月 1 日起至民國 87 年 12 月 31 日止

關鍵詞：氧化物、超導體、晶體結構、熱力學性質。

1. 摘要

以固態反應法製備一系列單相且具有三層鈦酸鈣結構的 $RBa_{1.5}Sr_{0.5}Cu_3O_y$ (R = La, Nd, Sm, Eu, Gd, Dy, Ho and Y)化合物。R 離子半徑大者(R = La, Nd)具四方晶相；其餘具正交晶相。$RBa_{1.5}Sr_{0.5}Cu_3O_y$ 的單位晶胞參數隨著 R 離子半徑大小而變。$RBa_{1.5}Sr_{0.5}Cu_3O_y$ 系列化合物中 R = Nd 時有最大的胞晶點；R = Sm 時，胞晶點反應所損失的重量最大；R=Eu 時有最大的熔融熱。胞晶點溫度高者熔融熱也比較大。隨著 R 離子變大，T_c 由 52 變高到 86K。

Keywords: oxide, superconductor, crystal structure. thermodynamic properties.

1. ABSTRACT

A series of single phase $RBa_{1.5}Sr_{0.5}Cu_3O_y$ (R = La, Nd, Sm, Eu, Gd, Dy, Ho and Y) compounds with a triple-perovskite unit-cell has been prepared by solid state reaction. Samples with a larger radius of the R ion (R = La and Nd) are tetragonal, while those with a smaller radius of the R ion (R = Sm, Eu, Gd, Dy, Ho and Y) are orthorhombic. The unit-cell parameters of $RBa_{1.5}Sr_{0.5}Cu_3O_y$ decrease monotonically with decreasing the radius of the R ion. Linear dependence of the variation of the *b* axis and unit-cell volume on the radius of the R ion is observed. Thermal analyses show that the peritectic transition temperature (t_p) exhibits a maximum as the radius of the R ion is decreased from R = La to R = Nd, and then gradually decreases with further decrease in the radius of the R ion. Similar behaviors are obtained in the change of the amount of oxygen loss (Δw) in the peritectic transition and the enthalpy of fusion (ΔH_f) with respect to the decrease in the radius of the R ion, but the maximum Δw and ΔH_f are observed for samples with R = Sm and Eu, respectively. It is also found that an increase in the ΔH_f is correlated with increasing t_p for the respective othorhombic and tetragonal phases of $RBa_{1.5}Sr_{0.5}Cu_3O_y$ compounds.

2. INTRODUCTION

Soon after the discovery of the 90 K $YBa_2Cu_3O_{7-\delta}$ superconductor (1), a series of 90 K $RBa_2Cu_3O_y$ (R = rare-earth, except Ce, Pr and Tb) superconductors is found (2,3). All of the 90 K $RBa_2Cu_3O_y$ superconductors exhibit an orthorhombic triple-perovskite structure (4,5), indicating that both T_c and the structure of $RBa_2Cu_3O_y$ are insensitive to the substitution of the R ion. On the other hand, if Ba is partially substituted with Sr in $YBa_2Cu_3O_{7-\delta}$, T_c of $YBa_{2-x}Sr_xCu_3O_y$ is decreased from 92 to 83 K as x is increased from 0 to 1 (6). Nevertheless, $YBa_{2-x}Sr_xCu_3O_y$ is still isostructural with $RBa_2Cu_3O_y$ (6). Interestingly, in $YBa_{2-x}Sr_xCu_3O_y$, if Y is replaced with Nd, the structure of the resulting $NdBa_{2-x}Sr_xCu_3O_y$ changes from orthorhombic to tetragonal as $x \geq 0.40$ (7). For x = 1 in $RBa_{2-x}Sr_xCu_3O_y$, the structure of $RBaSrCu_3O_y$ is related to the radius of the R ion (r_R). The $RBaSrCu_3O_y$ compounds with $r_R > r_{Dy}$ are tetragonal, while those with $r_R < r_{Dy}$ are othorhombic (8).

the particular R ion and the Sr content, the structure of $RBa_{2-x}Sr_xCu_3O_y$ can be orthorhombic or tetragonal. In this paper, with a fixed Sr content, a series of single phase $RBa_{1.5}Sr_{0.5}Cu_3O_y$ compounds with R = La, Nd, Sm, Eu, Gd, Dy, Ho and Y is prepared. Their preparation conditions, unit-cell parameters, phase transition and peritectic transition are studied.

2. EXPERIMENTAL

The $RBa_{1.5}Sr_{0.5}Cu_3O_y$ samples with R = La, Nd, Sm, Eu, Gd, Dy, Ho and Y were prepared by a standard solid state reaction. R_2O_3 was preheated at 1000 °C for 10 h and kept in desiccator prior to use. Stoichiometric amounts of R_2O_3, $SrCO_3$, $BaCO_3$ and CuO were weighed and ground thoroughly with a Retsch Spectro Mill Type MS for 30 min. The mixed powder was calcined at 950 - 960 °C for 14 h in a box furnace with three intermittent grindings and then reground and pressed into 1 cm diameter pellet. The resultant pellet was sintered at 900 - 960 °C for 12 h in a tube furnace. The optimum sintering temperatures for obtaining single phase varied with the R ion as listed in Table 1. After sintering, furnace temperature was lowered to 400 °C at a rate of 5 °C/min rate. All specimens were annealed at 400 °C for 12 h under flowing O_2 atmosphere and furnace cooled to room temperature. Purity of the samples was examined by a Mac Science MXP3 X-ray powder diffractometer equipped with a Cu K_α radiation, Ni-filter and graphite monochromater. The peaks of the X-ray diffraction (XRD) pattern were corrected with $K_{\alpha 2}$ elimination and calibrated with an internal Si standard. Unit-cell parameters were calculated using least squares refinement. Thermal analyses were performed with a Mac Science Thermal Analyzer System 001 equipped with TG-DTA 2020 and DSC 3320, and were carried under O_2 atmosphere with a flow rate of 25 $mL \cdot min^{-1}$ and a heating rate of 10 $°C \cdot min^{-1}$. TG-DTA was employed for measuring the peritectic transition temperature and the oxygen loss in the peritectic transition. DSC was used for dertermining the reaction enthalpy. The ionic radii of the R ions (r_R) with coordination number of 8 used in this paper were reported by Shannon (9).

3. RESULTS AND DISCUSSION

As listed in Table 1, there are differences in the preparation conditions for obtaining single phase $RBa_{1.5}Sr_{0.5}Cu_3O_y$ compounds. Lower oxygen partial pressure is employed to prepare samples with a larger R ion, but higher oxygen partial pressure is used for samples with a smaller R ion. For examples, $LaBa_{1.5}Sr_{0.5}Cu_3O_y$ is calcined under static air and sintered under flowing nitrogen atmosphere, but $HoBa_{1.5}Sr_{0.5}Cu_3O_y$ and $YBa_{1.5}Sr_{0.5}Cu_3O_y$ are synthesized under 1 atm oxygen pressure for the entire processes. Similar results are observed in the preparation of $LaBa_2Cu_3O_y$ and $YBa_2Cu_3O_y$ where the former is sintered under dried nitrogen atmosphere (10) and the latter is sintered under oxygen atmosphere (11).

Figure 1 shows the XRD patterns for all the single phase $RBa_{1.5}Sr_{0.5}Cu_3O_y$ compounds. As shown in Figure 1, phase transition in $RBa_{1.5}Sr_{0.5}Cu_3O_y$ is clearly seen by examining the intensity change in the Miller indices of (006), (200) and (020) planes of the XRD reflections in the range of $46 \leq 2\theta \leq 48°$ (11). Table 2 lists the diffraction angles of the Miller indices of (006), (200) and (020) planes of $RBa_{1.5}Sr_{0.5}Cu_3O_y$ compounds. For the larger R ion, R = La or Nd, the peak intensity of the (006) planes at 46.22° or 46.56° is smaller than that of the (200) and (020) planes at 46.52° or 46.74, indicating a tetragonal triple-perovskite phase. On the contrary, for the smaller rare-earth ion (R= Sm, Eu, Gd, Dy, Ho or Y), the peak intensity of the (006) and (020) planes at the smaller

angle is higher than that of the (200) planes at the larger angle, indicating an orthorhombic phase. The dependence of the structure on the radius of the R ion is also observed in $RBaSrCu_3O_y$ compounds (8).

Unit-cell parameters of $RBa_{1.5}Sr_{0.5}Cu_3O_y$ compounds are listed in Table 3. All of the parameters, *a*, *b*, *c* axis and volume, are gradually decreased with decreasing the ionic radius of the R ion as shown in Figure 2. A decrease in the *a*, *b*, and *c* axis is attributed mainly to a decrease in the radius of the R ion, resulting in a shrink in all the direction of the unit-cell. It should be noted that for the orthorhombic $RBa_{1.5}Sr_{0.5}Cu_3O_y$ compounds, the decreasing rate in the *a* axis is much greater than that in the *b* axis as shown in Figure 2(a). This is probably because the O5-site (0.5, 0, 0) in orthorhombic phase is empty which allows the squeeze of the *a* axis easier than that of the *b* axis where the corresponding O4 site (0, 0.5, 0) is almost fully occupied. A linear regression fitted to the volume of the $RBa_{1.5}Sr_{0.5}Cu_3O_y$ compounds with respect to the radius (r) of the R ion, obeying Vegard's law, is V = 114(3) + 0.56(3) r, where the correlation coefficient is 0.991, and numbers in parentheses are standard deviations referring to the last digit.

As shown in Table 3, the unit-cell axes and volume of $YBa_{1.5}Sr_{0.5}Cu_3O_y$ are smaller than those of $HoBa_{1.5}Sr_{0.5}Cu_3O_y$. This is unexpected taking consideration that ionic radius of Y is 1.019 Å and that of Ho is 1.015 Å for 8 coordination number (9) as in the R-site of the triple-perovskite center. Since all the unit-cell parameters of $YBa_{1.5}Sr_{0.5}Cu_3O_y$ are clearly smaller than those of $HoBa_{1.5}Sr_{0.5}Cu_3O_y$, it is conceivable that the ionic radius of Y is actually smaller than that of Ho in the triple-perovskite structure.

Orthorhombicity, 2(b – a)/(b + a), of the orthorhombic $RBa_{1.5}Sr_{0.5}Cu_3O_y$ compounds is increased with decreasing the radius of the R ion as can be seen in Table 3. It is clear that a transition to the tetragonal phase is induced for the larger R ion with $r_R \geq 1.109$ Å, while the orthorhombic phase is induced for the smaller R ion with $r_R \leq 1.079$ Å. In the $NdBa_{2-x.5}Sr_xCu_3O_y$ series where r_{Nd} =1.109 Å, orthorhombic phase is observed only for samples with $x \leq 0.40$ (7), but orthorhombic phase is observed for samples with $x \leq 1.50$ in $YBa_{2-x.5}Sr_xCu_3O_y$ series (6) where r_Y =1.019 Å. A large R ion causes an increase in all the *a*, *b*, *c* axis of the unit-cell. When *a* axis is increased, the possibility of filling oxygen atom in the O5-site is increased, resulting in a phase transition from orthorhombic to tetragonal.

Table 4 lists the peritectic transition temperature (t_p), the amount of the oxygen loss (Δw) in the peritectic transition and the enthalpy of fusion (ΔH_f) of $RBa_{1.5}Sr_{0.5}Cu_3O_y$ compounds. Figure 3 shows t_p versus the ionic radius of the R ion. Clearly, t_p is gradually increased to a maximum from R = La to R = Nd, and decreased thereafter as the radius of the R ion is further decreased. Similar results are observed for Δw and ΔH_f. However, as shown in Figures 4 and 5, the maximum Δw and ΔH_f are observed for R = Sm and R = Eu, respectively. Plotting the ΔH_f versus t_p in Figure 6, two lines are separately drawn for orthorhombic and tetragonal phases. An upward trend is observed in both phases, indicating that an increase in the heat of fusion is correlated with increasing t_p.

4. CONCLUSION

A series of $RBa_{1.5}Sr_{0.5}Cu_3O_y$ compounds is prepared. Unit-cell parameters are gradually decreased with decreasing the radius of the R ion. A phase transition from tetragonal to othorhombic is induced as the radius of the R ion is decreased. Peritectic transition temperature, the amount of the accompanied oxygen loss and the enthalpy of fusion show a maximum for samples with R = Nd, Sm and Eu, respectively. An increase in ΔH_f is correlated with increasing t_p for the respective tetragonal and othorhombic $RBa_{1.5}Sr_{0.5}Cu_3O_y$ compounds.

(1987).

ACKNOWLEDGMENT

The authors wish to thank National Science Council of ROC for the financial support of this work under grant NSC87-2113-M-032-007

REFERENCES

1.M. K. Wu, J. R. Ashburn, C. J. Torng, P. H.Hor, R. L. Meng, L. Gao, Z. J. Huang, Y. Q. Wang and C. W. Chu, *Phys. Rev. Lett.* **58**, 908 (1987).
2.P. H. Hor, R. L. Meng, Y. Q. Wang, L. Gao, Z. J. Huang, J. Bechtold, K. Forster and C. W. Chu, *Phys. Rev. Lett.* **58**, 1891 (1987).
3.K. N. Yang, Y. Dalichaouch, J. M. Ferreira, R. R. Hake, B. W. Lee, M. B. Maple, J. J. Neumeier, M. S. Torikachvili and H. Zhou, *MRS EA-11*, eds. D. U. Gubser and M. Schluter, 77 (1987).
4. M. A. Beno, L. Soderholm, D. W. Capone II, D. G. Hinks, J. D. Jorgensen, J. D. Grace, I. K. Schuller, C. U. Segre and K. Zhang, *Appl. Phys. Lett.* **51**, 57 (1987).
5.K. N. Yang, B. W. Lee, M. B. Maple and S. S. Landermann, *Appl. Phys. A* **46**, 229 (1988).
6.B. W. Veal, W. K. Kwok, A. Umezawa, G. W. Crabtree, J. D. Jorgensen, J. W. Downey, L. J. Nowicki, A. W. Mitchell, A. P. Paulikas and C. H. Sowers, *Appl. Phys. Lett.* **51**, 279 (1987).
7.C. W. Cheng, *Master thesis*, Tamkang University, Tamsui, Taiwan 1996.
8.X. Z, Wang, B. Hellebrand and D. Bauerle, *Physica C* **200**, 12 (1992).
9.R. D. Shannon, *Acta Crystallogr. A* **32**, 751 (1976).
10.T. Wada, N. Suzuki, S.-i. Uchida and S. Tanaka, *Phys. Rev. B* **39**, 9126 (1989); T. Wada, T. Sakurai, N. Suzuki, *Phys. Rev. B* **41**, 209 (1990);
11. A. M. Kini, U. Geiser, H.-C. I. Kao, K. D. Carlson, H. H. Wang, M. R. Monaghan and J. M. Williams, *Inorg. Chem.* **26**, 1836

TABLE 1
Preparation Conditions of the $RBa_{1.5}Sr_{0.5}Cu_3O_y$ Compounds

R	Atmosphere		
	Calcination (°C)	Sintering (°C)	Annealing (°C)
La	950/static air	960/flowing N_2	400/flowing O_2
Nd	960/static air	920/flowing O_2	400/flowing O_2
Sm, Eu, Gd, Dy	950/static air	900/flowing O_2	400/flowing O_2
Ho	950/flowing O_2	930/flowing O_2	400/flowing O_2
Y	950/flowing O_2	950/flowing O_2	400/flowing O_2

TABLE 2
The 2θ Angle of (006), (200), and (020) Bragg Diffraction for $RBa_{1.5}Sr_{0.5}Cu_3O_y$ Compounds

R	(006)	(200) (020)	(006) (020)	(200)	Phase
La	46.22	46.52			tetragonal
Nd	46.56	46.74			tetragonal
Sm			46.64	47.18	orthorhombic
Eu			46.70	47.32	orthorhombic
Gd			46.76	47.46	orthorhombic
Dy			46.82	47.66	orthorhombic
Ho			46.88	47.74	orthorhombic
Y			46.90	47.80	orthorhombic

TABLE 3
Unit-Cell Parameters and Orthorhombicity of $RBa_{1.5}Sr_{0.5}Cu_3O_y$ Compounds

R	R^{3+} radius (Å)	a (Å)	b (Å)	c (Å)	V (Å)	Orthorhombicity
La	1.160	3.8982(6)	-	11.759(3)	178.68(7)	0
Nd	1.109	3.8887(2)	-	11.689(1)	176.76(3)	0
Sm	1.079	3.8424(8)	3.8836(8)	11.657(4)	173.95(8)	0.0106
Eu	1.066	3.8361(4)	3.8830(6)	11.655(3)	173.61(5)	0.0121
Gd	1.053	3.8285(7)	3.8782(8)	11.654(4)	173.03(8)	0.0129
Dy	1.027	3.8068(9)	3.8743(9)	11.632(5)	171.55(9)	0.0176
Ho	1.015	3.8042(4)	3.8739(4)	11.610(2)	171.10(4)	0.0181
Y	1.019	3.7976(10)	3.8725(10)	11.606(5)	170.68(9)	0.0196

Numbers in parentheses are standard deviations referring to the last digit.

TABLE 4
Peritectic Transition Temperature (t_p), the Accompanied Oxygen Loss (Δw), and Enthalpy of Fusion (ΔH_f) of $RBa_{1.5}Sr_{0.5}Cu_3O_y$ Compounds

R	t_p (°C)	$\Delta w \cdot mol^{-1}$)	ΔH_f ($kJ \cdot mol^{-1}$)
La	1092	0.324	140
Nd	1117	0.469	211
Sm	1112	0.475	243
Eu	1103	0.430	245
Gd	1090	0.455	225
Dy	1064	0.380	206
Ho	1055	0.394	179
Y	1060	0.322	159

TABLE 5

$T_{c(zero)}$, 290 K Resistivity, and the Resistivity Ratio of $RBa_{1.5}Sr_{0.5}Cu_3O_y$ Compounds

R	$T_{c(zero)}$ (K)	ΔT_c (K)	(ρ290)(mΩ·cm)	(ρ100)/(ρ290)
La	52.4	8.8	9.76	1.29
Nd	56.4	10.2	6.70	1.24
Sm	70.7	8.3	3.37	1.22
Eu	76.8	6.4	4.03	1.25
Gd	85.6	1.7	2.92	1.46
Dy	86.5	1.1	2.25	1.58
Ho	86.8	1.5	1.43	1.76
Y	87.4	2.3	1.32	1.89

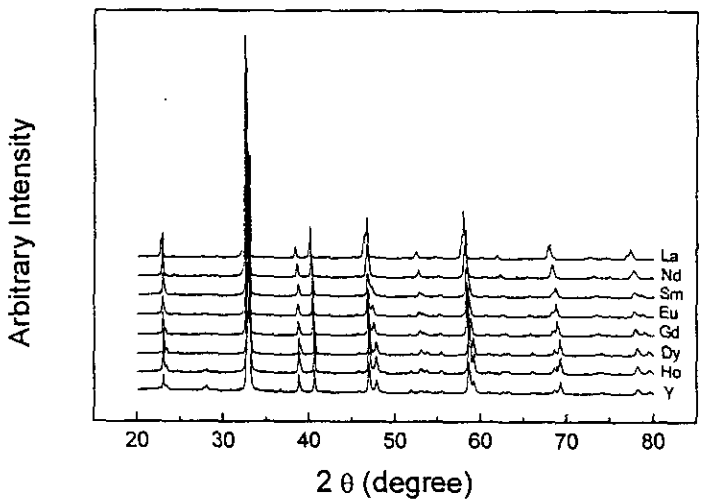

FIG. 1

XRD patterns of single-phase $RBa_{1.5}Sr_{0.5}Cu_3O_y$ compounds with R = La, Nd, Sm, Eu, Gd, Dy, Ho, and Y.

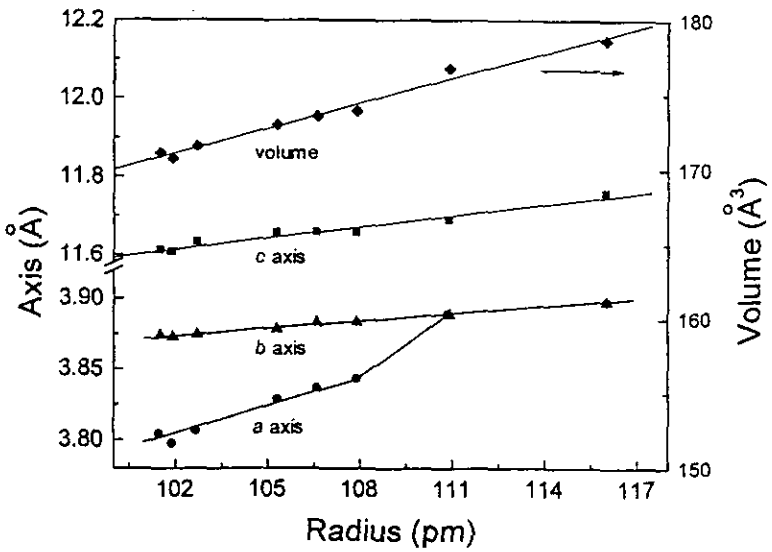

FIG. 2

Unit-cell parameters (*a*, *b*, and *c* axes and volume) vs. ionic radius of the R ion for $RBa_{1.5}Sr_{0.5}Cu_3O_y$ compounds.

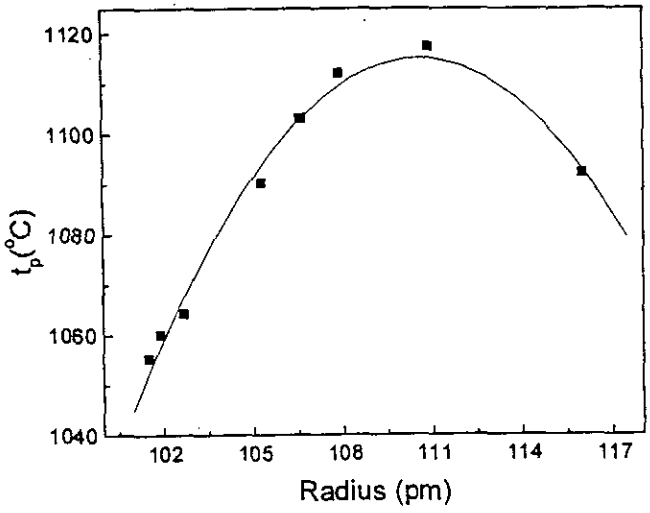

FIG. 3

t_p vs. ionic radius of the R ion for $RBa_{1.5}Sr_{0.5}Cu_3O_y$ compounds.

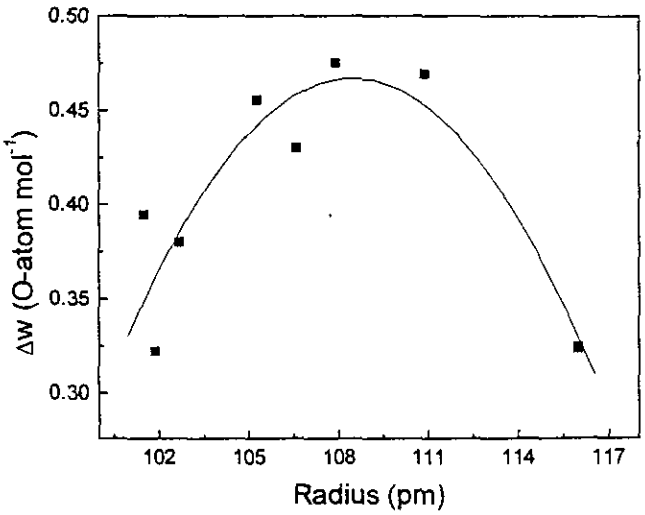

FIG. 4

Δw vs. ionic radius of the R ion for $RBa_{1.5}Sr_{0.5}Cu_3O_y$ compounds.

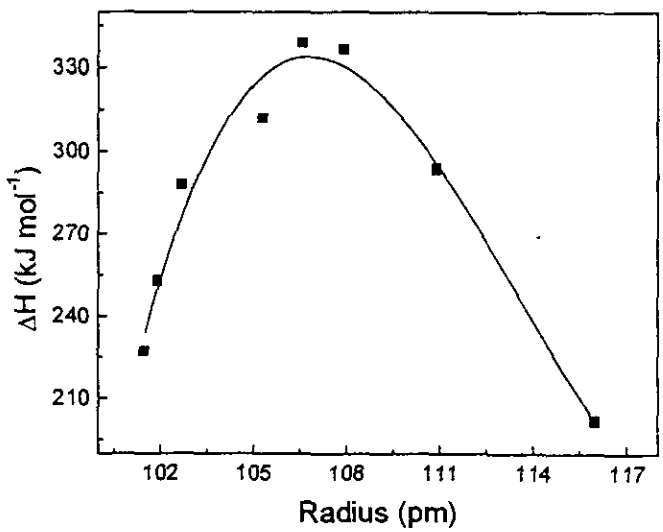

FIG. 5

ΔH_f vs. ionic radius of the R ion for $RBa_{1.5}Sr_{0.5}Cu_3O_y$ compounds.

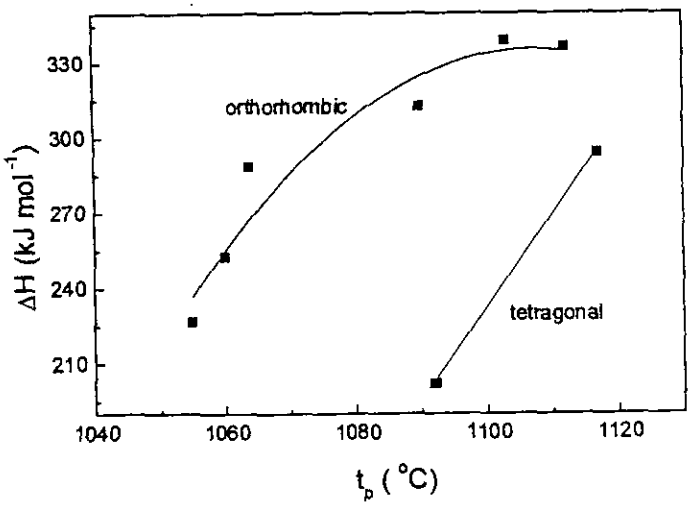

FIG. 6
ΔH_f vs. t_p of $RBa_{1.5}Sr_{0.5}Cu_3O_y$ compounds.

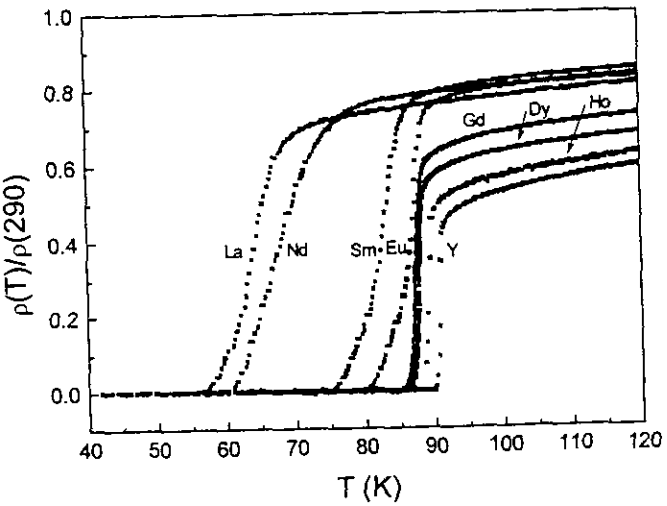

FIG. 7
Temperature-dependent normalized resistivity of $RBa_{1.5}Sr_{0.5}Cu_3O_y$ compounds.